CONF-9609243--8

SAND97-0058C
SAND--97-0058C

COMPARISON OF CALCULATED AND EXPERIMENTAL DOSIMETRY ACTIVITIES FOR BENCHMARK NEUTRON FIELDS*

P. J. Griffin
Sandia National Laboratories, Org. 9363, MS 1146
Albuquerque, NM 87185-1146, USA
pjgriff@sandia.gov

ABSTRACT

An analysis of the calculated-to-experimental (C/E) ratios is presented for neutron benchmark fields. The sources of uncertainty are described and quantified. The consistency of the data with the reported uncertainties is examined.

1. Introduction

New dosimetry cross-section evaluations have been made available to the reactor community. Most dosimetry-quality evaluations include a section (File 33) that defines the uncertainty and covariance matrix for the dosimetry reaction cross section. This paper compares the latest computed cross-section activities for benchmark neutron fields with experimental data. Uncertainty data is usually reported with experimental measurements. This work also presents uncertainty data for the calculated activities. The calculated uncertainty values include a full uncertainty propagation using the cross-section evaluation, energy-dependent covariance data as well as the uncertainty attributed to the knowledge of the neutron spectrum.

2. Neutron Fields

This paper presents results for a variety of neutron fields. Neutron fields can be divided into several different categories. The reactor dosimetry community has identified three categories of benchmark fields[1]; standard fields, reference fields, and controlled fields. Standard benchmark fields are very well-characterized neutron sources that are maintained by national standards organizations for calibration purposes and include the ^{252}Cf spontaneous fission neutron field and the ^{235}U thermal fission spectrum. Standard neutron field spectra generally have an analytic basis for the spectrum shape and have been characterized by time-of-flight detection methods. Reference fields are well-characterized, stable, and reproducible neutron sources used by specific communities to ensure consistency in the determination of performance metrics. Well-known reference fields include the MDRF[2] and CFRMF[3] neutron fields. The SPR-III central cavity[4] is used as a reference field for assessing the radiation damage to electronics and is included in this category. Controlled fields are engineering benchmarks that are characterized for the purpose of developing and

*This work was performed at Sandia National Laboratories, which is operated for the U.S. Department of Energy under contract DE-AC04-94AL85000.

DISCLAIMER

validating experimental and/or calculational dosimetry techniques. Engineering benchmarks used by the reactor pressure vessel surveillance community include the PCA/PSF, VENUS, and NESDIP experiments. In this analysis the ACRR central cavity[5] is included as an engineering benchmark field for pool-type research reactors.

A 1/E spectrum and a thermal Maxwellian spectrum are commonly considered to be benchmark fields. These neutron fields are useful for dosimetry purposes when dealing with a nonthreshold reaction. A 1/E component is introduced to a neutron field by neutron scattering. A fast fission and a thermal component are typically also present. When the dosimeter of interest is based on a nonthreshold neutron reaction, the large thermal and resonance region cross section dominate and the fast component can usually be ignored. The thermal component is typically removed by using a cadmium cover. The neutron scattering field is described by a 1/E shape only when hydrogen is used as a moderator and the system has no leakage term. For other neutron scattering materials, the scattered field can be approximately described as a $1/E^{(1+\alpha)}$ field[6]. A thermal Maxwellian is a component of most fields where neutron scattering occurs. Neutron thermal columns are created by introducing a large moderating region to a fission neutron source. These fields are typically characterized by the ratios of neutron activation for bare and cadmium-covered neutron sensors. When 1/E and thermal fields are used with neutron sensors having a low thermal neutron sensitivity and a high fast neutron sensitivity, care must be taken to provide estimates of the sensor response from the "contaminant" fast neutron components in the neutron spectrum.

The 14-MeV neutron field is also considered to be a standard neutron field. This neutron field is useful to the materials damage assessment for the fusion community but is not used by the reactor community. This mono-energetic neutron field is useful since it can be easily produced by the $^{3}H(^{2}H,n)^{4}He$, or DT, reaction. Most DT sources use the large 107 keV resonance in the cross section and produce neutrons with energies between 13.9 and 14.9 MeV.

3. Experimental Data

No new experimental data are presented as part of this paper. Experimental data are taken from the literature and are typically accompanied by an uncertainty estimate. For standard fields there is a wealth of experimental measurements and careful evaluations of the existing data have been made[7,8,9,10]. The 14-MeV neutron cross-section measurement data are available from a number of sources[10,11] and the consistency of reactions used as dosimeters in 14-MeV fields has been studied[12]. Spectrum covariance data are rarely available for reference or engineering benchmark field neutron spectra. Sensitivity analyses are usually available for reference fields.

4. Calculated Cross-Section Data

High fidelity cross sections for reactions of interest as dosimeters are available from several sources including the ENDF/B, JEF, JENDL, BROND, and CENDL libraries of evaluated cross sections. The IRDF[13] and GLUCS[14] libraries are dosimetry-specific collections of evaluated cross sections. A comparison of dosimetry cross sections from these sources has been made. The result of this comparison is the SNLRML cross-section compendium[15]. The SNLRML cross sections have been drawn from the existing sets of cross-section evaluations and represent this authors view of the highest-quality community-consensus cross sections for dosimetry reactions. The cross sections and cross section

covariance data used in this paper have been taken from the SNLRML. In most cases when a cross section is given in both the IRDF90[13] and SNLRML collections, they are identical.

5. Uncertainty Metrics

The proper treatment and propagation of covariance data is crucial to the understanding of the calculated uncertainty data for high fidelity dosimetry reactions. Simply taking a spectrum/cross-section weighted average standard deviation is not a sufficient approach[16]. The new $^{32}S(n,p)^{32}P$ cross section from the GLUCS-91 and IRDF-90 library, for example, gives uncertainty data in a very fine energy grid with detailed correlation data. If the correlation information is neglected, the average spectrum-averaged cross-section uncertainty in a fast burst reactor is 19%. This represents a significant increase over the 7% uncertainty from the older IRDF-82 library. The higher uncertainty is due to the finer resolution of the uncertainty data and the neglect of a proper treatment of the correlations. When the GLUCS-91 uncertainty data is properly propagated, the sulfur spectrum-averaged cross section uncertainty in a fast-burst reactor neutron spectrum is 6.5%. The overall uncertainty estimate does not significantly change from the IRDF-82 library results. However, if the detailed correlation information in the new high fidelity covariance matrices is neglected, the spectrum-averaged uncertainty can appear to change and be seriously overstated. A comparison of the fully-propagated, average, and observed cross-section uncertainty for dosimetry reactions can be found in Reference 16.

In some cases, such as the ^{252}Cf field, covariance data is available for the neutron spectrum. In these cases, the uncertainty in the neutron spectrum data (assumed to be independent of the cross section data) is also treated in calculating the spectrum-averaged uncertainty of the activity. The treatment of covariance data for the other spectra is discussed in subsections 6.1 through 6.6.

6. Comparison of Experimental and Calculated Cross Sections

Using existing experimental data, this paper compares the C/E (calculated-to-experimental) ratios for dosimetry reactions in benchmark fields. These data will be used to update the benchmark field activity data in several ASTM standards (E 261, E 262, E 481). These data also serve to draw the attention of the dosimetry community to reactions where the deviation of the C/E ratio from unity exceeds the inferred uncertainty in the ratio.

6.1. ^{252}Cf Spontaneous Fission Standard Field

Table 1 compares the experimental and calculated spectrum-averaged cross sections in this neutron field for a range of important dosimetry reactions and provides fully propagated measures for the components of the uncertainty. The uncertainty is given in terms of a percentage of the cross-section value and is placed in parenthesis after the value. The calculated uncertainty has two terms in parenthesis, the first term represents the uncertainty attributed to the cross section, the second term represents the uncertainty attributed to the knowledge of the source spectrum. Figure 1 plots the resulting C/E (calculated over experimental) ratios and the uncertainty in this ratio (at the 1σ level) versus the median neutron energy for the sensor response in this neutron field. The majority of this experimental data is taken from the data evaluation work by Mannhart[17,18]. Boldeman[19] provides a good review of the measurement data in this benchmark field. The ^{252}Cf spontaneous fission

spectrum and covariance matrix were taken from the ENDF/B-VI files, MAT=9861.

Although much data is available for cross sections in this standard field, little of the data is for neutron capture, (n,γ), reactions. Because this is a pure fission neutron spectrum with no significant thermal neutron component, the C/E ratios for capture reactions have a median energy of ~ 0.2 MeV and a large C/E uncertainty. The failure of two of the five capture C/E ratios to be within three sigma of unity is a concern. Possible explanations of this failure include too optimistic an estimate on the high energy portion of the cross section for neutron capture reactions, or the presence of a contaminant scattered neutron component in those fields where the experimental neutron capture data was obtained.

Table 1. Fission-Spectrum-Averaged Cross Sections for Threshold Activation Detectors

Reaction	^{252}Cf Spontaneous Fission Field			^{235}U Thermal Fission Field		
	Calc. (mb)	Obs. (mb)	C/E	Calc. (mb)	Obs. (mb)	C/E
^{197}Au(n,γ)^{198}Au	74.17 (1.22%, 1.05%)	76.86 (1.59%)	0.965 (2.26%)	75.05 (1.18%, 5.64%)	83.5 (6.0%)	0.899 (8.32%)
^{59}Co(n,γ)^{60}Co	4.780 (4.14%, 2.66%)	6.97 (5.0%)	0.686 (7.02%)	4.833 (4.18%, 8.75%)	---	---
^{23}Na(n,γ)^{24}Na	0.272 (13.0%, 1.23%)	0.335 (4.0%)	0.811 (13.67%)	0.271 (13.2%, 5.44%)	---	---
^{63}Cu(n,γ)^{64}Cu	10.40 (8.55%, 0.745%)	10.45 (3.24%)	0.995 (9.17%)	10.48 (8.63%, 4.73%)	9.3 (15.0%)	1.127 (17.9%)
^{115}In(n,γ)^{116m}In	154.15 (4.33%, 0.376%)	125.7 (2.23%)	1.23 (4.88%)	157.42 (4.36%, 4.42%)	134.5 (4.0%)	1.170 (5.97%)
^{235}U(n,f)FP	1218.2 (0.32%, 0.08%)	1210.0 (1.2%)	1.007 (1.24%)	1215.85 (0.32%, 4.04%)	1216.0 (1.6%)	1.000 (4.36%)
^{239}Pu(n,f)FP	1789.46 (0.41%, 0.07%)	1812.0 (1.37%)	0.988 (1.43%)	1788.4 (0.41%, 4.03%)	1832.0 (3.0%)	0.976 (5.06%)
^{237}Np(n,f)FP	1335.1 (9.2%, 0.23%)	1361.0 (1.58%)	0.981 (9.34%)	1330.1 (9.33%, 4.31%)	1344.0 (4.0%)	0.9897 (11.0%)
^{103}Rh(n,n')^{103m}Rh	714.45 (3.08%, 0.27%)	757.0 (4.0%)	0.944 (5.06%)	706.02 (3.1%, 4.14%)	733.0 (5.2%)	0.963 (7.33%)
^{115}In(n,n')^{115m}In	189.8 (2.16%, 0.38%)	197.6 (1.3%)	0.961 (2.55%)	186.35 (2.17%, 4.17%)	190.3 (3.84%)	0.979 (6.07%)
^{93}Nb(n,n')^{93m}Nb	142.65 (3.04%, 0.36%)	149.0 (7.0%)	0.957 (7.64%)	139.97 (3.06%, 4.14%)	146.2 (8.6%)	0.957 (10.0%)
^{238}U(n,f)FP	315.39 (0.53%, 0.40%)	325.7 (1.63%)	0.968 (1.76%)	306.23 (0.53%, 4.21%)	309.0 (2.6%)	0.991 (4.98%)
^{232}Th(n,f)FP	78.52 (5.07%, 0.43%)	89.4 (3.03%)	0.878 (5.92%)	75.33 (5.09%, 4.13%)	81.0 (7.0%)	0.930 (9.59%)
^{47}Ti(n,p)^{47}Sc	19.38 (3.76%, 0.63%)	19.29 (1.66%)	1.005 (4.16%)	17.95 (3.7%, 4.26%)	19.0 (7.4%)	0.9456 (9.31%)
^{31}P(n,p)^{31}Si	30.67 (3.54%, 0.707%)	35.2	0.871	28.36 (3.54%, 4.58%)	33.5 (6.0%)	0.847 (8.34%)
^{32}S(n,p)^{32}P	70.44 (4.01%, 0.75%)	72.62 (3.5%)	0.970 (5.38%)	64.69 (4.0%, 4.86%)	66.8 (5.54%)	0.968 (8.39%)
^{58}Ni(n,p)^{58}Co	115.3 (2.40%, 0.73%)	117.6 (1.3%)	0.981 (2.83%)	105.7 (2.43%, 4.52%)	108.5 (5.0%)	0.974 (7.16%)
^{64}Zn(n,p)^{64}Cu	42.09 (4.79%, 0.79%)	40.63 (1.64%)	1.036 (5.12%)	38.40 (4.72%, 4.81%)	29.9 (5.35%)	1.284 (8.60%)
^{54}Fe(n,p)^{54}Mn	88.12 (2.14%, 0.79%)	86.92 (1.34%)	1.014 (2.65%)	80.18 (2.17%, 4.69%)	80.5 (2.86%)	0.996 (5.91%)
^{59}Co(n,p)^{59}Fe	1.692 (4.08%, 1.14%)	1.692 (2.49%)	1.000 (2.74%)	1.412 (4.11%, 5.20%)	1.41 (3.55%)	1.001 (7.52%)
^{27}Al(n,p)^{24}Mg	4.748 (2.94%, 1.14%)	4.885 (2.14%)	0.972 (3.81%)	3.977 (3.06%, 5.28%)	3.95 (5.06%)	1.007 (7.93%)
^{46}Ti(n,p)^{46}Sc	12.56 (2.45%, 1.18%)	14.09 (1.76%)	0.891 (3.24%)	10.43 (2.46%, 5.40%)	11.6 (3.45%)	0.899 (6.86%)
^{60}Ni(n,p)^{60}Co	2.493 (10.1%, 1.37%)	2.39 (5.0%)	1.043 (11.34%)	1.935 (10.3%, 6.04%)	---	---
^{63}Cu(n,α)^{60}Co	0.678 (2.83%, 1.38%)	0.689 (1.98%)	0.984 (3.72%)	0.521 (2.85%, 6.05%)	0.50 (11.0%)	1.042 (12.9%)
^{56}Fe(n,p)^{56}Mn	1.370 (2.23%, 1.45%)	1.466 (1.77%)	0.934 (3.20%)	1.029 (2.33%, 6.58%)	1.09 (3.67%)	0.944 (7.89%)
^{24}Mg(n,p)^{24}Na	2.162 (2.24%, 1.57%)	1.998 (2.42%)	1.082 (3.65%)	1.553 (2.34%, 7.12%)	1.38 (5.1%)	1.126 (9.07%)
^{59}Co(n,α)^{56}Mn	0.216 (2.73%, 1.54%)	0.222 (1.86%)	0.974 (3.64%)	0.1548 (2.80%, 6.61%)	0.161 (4.35%)	0.961 (7.95%)
^{48}Ti(n,p)^{48}Sc	0.3968 (2.56%, 1.55%)	0.4251 (1.89%)	0.933 (3.54%)	0.2816 (2.54%, 6.66%)	0.302 (3.31%)	0.933 (7.86%)
^{27}Al(n,α)^{23}Na	1.04 (1.36%, 1.61%)	1.017 (1.47%)	1.019 (2.57%)	0.727 (1.40%, 6.95%)	0.706 (3.97%)	1.030 (8.13%)
^{197}Au(n,2n)^{196}Au	5.744 (4.20%, 1.99%)	5.511 (1.83%)	1.042 (4.99%)	3.474 (4.41%, 8.39%)	3.50 (3.71%)	0.993 (10.2%)
^{93}Nb(n,2n)^{92m}Nb	0.779 (2.78%, 2.20%)	0.749 (5.07%)	1.040 (6.19%)	0.4459 (2.99%, 8.17%)	0.4796 (6.10%)	0.930 (1.06%)
^{127}I(n,2n)^{126}I	2.355 (17.14%, 2.26%)	2.071 (2.75%)	1.137 (17.5%)	1.329 (17.16%, 8.15%)	1.04 (6.19%)	1.278 (20.0%)
^{65}Cu(n,2n)^{64}Cu	0.6782 (2.24%, 2.85%)	0.6587 (2.24%)	1.030 (4.26%)	0.3466 (2.37%, 9.74%)	---	---
^{55}Mn(n,2n)^{54}Mn	0.4816 (12.3%, 3.01%)	0.4079 (2.34%)	1.181 (12.88%)	0.2417 (13.4%, 10.26%)	0.202 (5.0%)	1.197 (17.6%)
^{59}Co(n,2n)^{58}Co	0.4228 (2.61%, 3.17%)	0.4055 (2.52%)	1.043 (4.82%)	0.2082 (2.89%, 10.8%)	0.202 (2.97%)	1.031 (11.6%)
^{63}Cu(n,2n)^{62}Cu	0.2091 (1.65%, 4.05%)	0.1845 (3.89%)	1.133 (5.85%)	0.0958 (1.79%, 9.97%)	0.122 (9.84%)	0.785 (14.1%)
^{19}F(n,2n)^{18}F	0.0172 (2.63%, 4.31%)	0.01613 (3.4%)	1.070 (6.09%)	0.0078 (2.92%, 9.97%)	---	---
^{90}Zr(n,2n)^{89}Zr	0.2377 (1.77%, 4.81%)	0.2212 (2.9%)	1.075 (5.89%)	0.1037 (1.88%, 10.3%)	0.103 (3.88%)	1.006 (11.1%)
^{58}Ni(n,2n)^{57}Ni	0.00926 (2.54%, 6.04%)	0.00896 (3.59%)	1.033 (7.47%)	0.00379 (2.61%, 11.5%)	0.0036 (7.0%)	1.052 (13.7%)

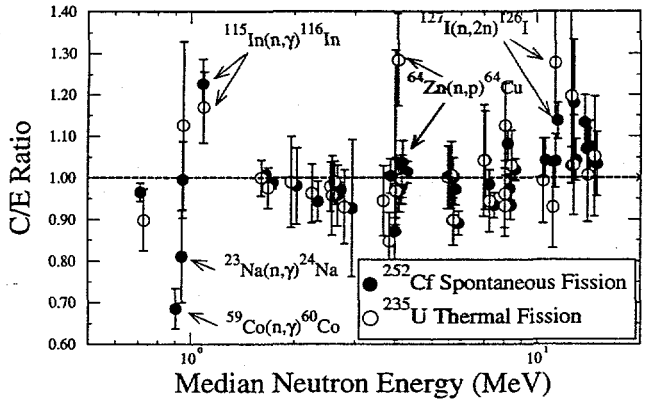

Figure 1. C/E For Standard Fission Benchmark Fields

The fact that most of the C/E data is below unity is consistent with the presence of a scattered component in the measurement field. The scattered neutron component of ^{252}Cf sources at national standard facilities has been bounded by observing the bare and cadmium-covered capture reactions[9], but the inferred cross-section data from these tests does not appear to have been published. Another possibility is that contaminant scattered neutrons may have been present in cross-section measurements used to support the calculated cross sections for the high energy portion of the neutron capture reactions. However, the presence of this contaminant should have been considered in placing bounds on the cross-section uncertainty.

A distinct trend is seen in the high energy region (12 - 15 MeV) of the C/E data in Fig. 1. The fact that a single data point has uncertainty bounds that do not include unity only indicates that a specific cross section may have problems. However, when several reactions show the same trend in the same energy region, suspicion is placed on the characterization of the neutron spectrum. The high energy part of the ^{252}Cf spectrum is already assigned a fairly large uncertainty. The literature[20] shows that small changes in the Madland-Nix nuclear potential parameters can result in large changes in the high energy part of the ^{252}Cf fission neutron spectrum. The data in Fig. 1 suggests that the high energy component of the ^{252}Cf fission neutron spectrum is too large and indicates that the uncertainty in the high energy component is underestimated.

When the C/E ratios in the ^{252}Cf neutron field are considered as an aggregate, the data is seen to be discrepant. The chi-squared per degree of freedom, χ^2/f, for the entire dataset is 3.3. If the ^{59}Co(n,γ)^{60}Co reaction is removed, χ^2/f is 2.3. No other single discrepant datapoint has been identified where the χ^2/f is significantly improved with its removal. The ^{252}Cf data and the assigned uncertainties need to be reviewed in light of this chi-squared.

6.2. ^{235}U Thermal Fission Standard Field

The ^{235}U thermal fission standard field is not as easily created or measured as the ^{252}Cf field. Consequently, there is less experimental data in this field and larger uncertainties. Most of the ^{235}U thermal fission experimental data seen in Table 1 are taken from References 7 and 10. The ^{235}U spectrum is taken from ENDF/B-VI files and the covariance data are taken from Reference 21.

Figure 1 shows the C/E ratios for this standard field. Unlike the ^{252}Cf case, there is no obvious discrepancy in the high energy part of this standard field, nor in the aggregate C/E data. This difference could be attributed to the fewer high energy experimental data points or to the higher uncertainty on the datapoints. The χ^2/f for the C/E data is 0.977.

Data are only available for three neutron capture reactions in this standard field. Of these

capture reactions only the $^{115}In(n,\gamma)^{116}In$ C/E ratio shows bounds that are significantly outside unity. The C/E ratio for this reaction in the ^{235}U field is 1.17+/- 5.97% and in the ^{252}Cf field is 1.23 +/- 4.88%. This suggests that the $^{115}In(n,\gamma)^{116}In$ high energy cross section is overestimated and the uncertainty in the cross section is underestimated

Another reaction that shows an overestimated cross section and an underestimated uncertainty in both the ^{235}U and ^{252}Cf standard environments is the $^{127}I(n,2n)^{126}I$ reaction. The $^{46}Ti(n,p)^{46}Sc$ and $^{31}P(n,p)^{31}S$ reactions show consistent trends of an underestimated cross section with marginal uncertainty bounds.

6.3. 14-MeV Field

Data are available for many neutron sensors in 14-MeV neutron fields. However, the energy of the monoenergetic neutron field varies with the accelerator voltage and the angle of the detector relative to the deuteron source particle. Studies of the systematics of the (n,p) and (n,α) reactions in this region have been made and the consistency of experimental measurements in this region have been made. In the case of a 14-MeV field, the neutron energy is usually monoenergetic with a full width at half maximum of about 200 keV. This shape has been adopted for reporting calculated cross sections for this field in this paper. The source uncertainty is usually associated with the detector angle and the accelerator voltage. As a consequence, the DT cross-section data are not always reported with the same neutron energy. The data reported in Figure 2 come from various sources and the data are reported for energies from 14.7 to 14.9 MeV. The proper source uncertainty term for these data is a probability density function or pdf for the neutron energy. A pdf has been constructed which represents the variation of energy in the available cross-section data. Using this pdf and the shape of the cross section in the region around the mean energy of 14.7 MeV, a standard deviation for the neutron-source induced uncertainty in the resulting cross section has been constructed. This source-induced standard deviation and the uncertainty attributed to the knowledge of the cross section are reflected in Figure 2.

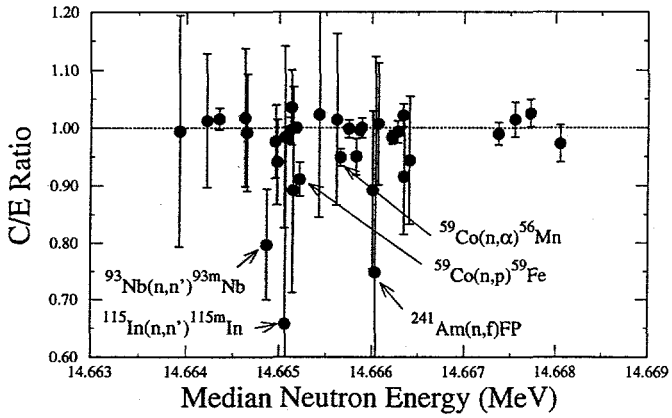

Figure 2. C/E For 14-MeV Benchmark Neutron Field

Since 14-MeV data are relatively easily acquired, this energy plays an important role in the normalization of calculated neutron cross-section data. Thus one would expect that the C/E ratios would be close to unity and the uncertainty bounds for threshold reactions should be small. The C/E ratios for important dosimetry reactions confirm this expectation. The x-axis in Figure 2 is the median response energy. It varies from reaction to reactions based on the shape of the cross section near 14.7 MeV. In general, calculated cross sections and experiments agree in this neutron field and have relatively small uncertainty bounds. The χ^2/f for the C/E data is 1.06.

6.4. *1/E and Thermal Maxwellian Fields*

1/E and thermal Maxwellian neutron fields are idealized benchmark fields. Any source uncertainty must be attributed to actual implementations of these fields and not to the fields themselves. Thus C/E ratios only make sense when referring to a specific facility. However, the uncertainty due to the knowledge of the cross sections themselves in these fields is important in the selection of dosimetry sensors. Tables showing the uncertainty of various nonthreshold dosimetry reactions in these neutron fields are currently being incorporated into ASTM standards E261 and E262.

6.5. *SPR-III Central Cavity Reference Field*

The SPR-III central cavity environment has been described in other publications[22,23]. Figure 3 summarizes the cross section and uncertainty data for this reference field. These data include covers that were used on the dosimeters. Covers are very useful in shifting the region of response for the sensor. Reference 22 provides details describing the covers and the modified response functions and response covariance matrices. The spectrum was determined using an iterative unfold technique with the SNL-SAND-II code[24]. The spectrum covariance was determined by statistically perturbing the foil activities and the trial spectrum within the uncertainty bounds for the input parameters. Monte Carlo calculations of the neutron spectrum show good agreement with the SAND-II unfolded spectrum. The covariance matrix determined with the least squares-based LSL-M2 code is also in good agreement with that determined from the SAND-II perturbation approach.

The C/E uncertainty bounds in Fig. 3 generally include unity. This is expected since foil activation data was the primary input in the spectrum determination. The χ^2/f is 1.6 when data from all 38 available reactions are included. If discrepant data for the ^{59}Co(n,γ), ^{55}Mn(n,γ) and ^{238}U(n,f) reactions are eliminated, the χ^2/f is 1.02. Since the reference field has a modest 1/E and thermal neutron component, the median energy for each sensor response is seen to be much more spread out than for the fast fission ^{235}U and ^{252}Cf fields.

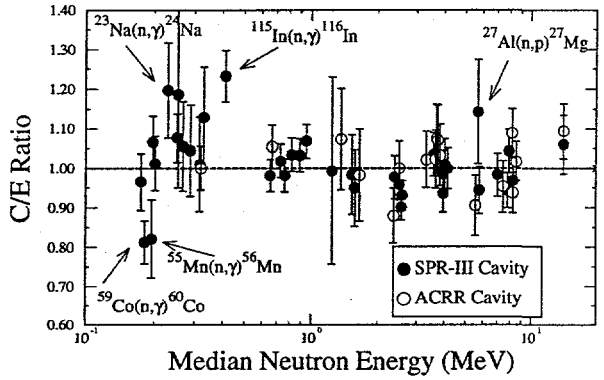

Figure 3. SPR-III and ACRR Neutron Benchmark Fields

6.6.ACRR Central Cavity Controlled Environment

The ACRR central cavity field is included in this analysis to represent the situation of a well-moderated reactor spectrum. This spectrum was determined by the same techniques used for the SPR-III central cavity, but a complete sensitivity analysis has not been performed. Figure 3 shows C/E ratios for this environment. Whereas the SPR-III spectrum showed some spread in the median sensor response, the sensor response in the ACRR environment clusters into two distinct regions, one from 0.1 - 2.0 MeV, the second from 1 eV - 1 keV. The use of ^{10}B-enriched covers and the use of the fission and silicon 1-MeV sensor are very important in determining a spectrum for this environment. This benchmark field has a χ^2/f of 0.607 with 26 degrees of freedom.

7. Conclusion

This paper has presented an analysis of the C/E ratios for benchmark neutron environments. Although C/E data have been previously presented, this analysis utilizes updated calculated cross sections using the latest dosimetry-quality cross section evaluations and provides the first complete uncertainty analysis of the C/E data. The results show a consistency between calculated and measured dosimetry reactions in four out of five benchmark fields that have been analyzed. The ^{252}Cf benchmark field being the only exception. In addition, analysis of the C/E data for the ^{252}Cf benchmark field suggest some problems with the high energy portion of the ^{252}Cf fission neutron spectrum.

8. References

[1] *Neutron Cross Sections for Reactor Dosimetry*, IAEA, Laboratory Activities, 1978, **Vol. 1**, p. 62.

[2] A. I. Hawari, et al., *Reactor Dosimetry*, ASTM STP 1228, 1994, pp. 401-410.

[3] J. W. Rogers, D. A. Millsap, Y. D. Harker, *Nuclear Technology*, **Vol. 25**, Feb. 1975, pp. 330-348.

[4] J. G. Kelly, P. J. Griffin, *IEEE Trans. Nucl. Science*, **Vol. NS-40**, No. 6, 1993, pp. 1418-1425.

[5] P. J. Griffin, J. G. Kelly, D. W. Vehar, *Updated Neutron Spectrum Characterization of SNL Baseline Reactor Environments,* SAND93-2554, Sandia National Laboratories, Albuquerque, NM, 1994.

[6] T. Bereznal, T. D. McMahon, *Journal of Radioanalytical Chemistry*, **Vol. 45**, 1978, pp. 423-434.

[7] A. Fabry, et al., *Neutron Cross Sections for Reactor Dosimetry*, International Atomic Energy Agency, report IAEA-208, **Vol. 1**, 1978, pp. 233-263.

[8] I. Kimura, et al., *Neutron Cross Sections for Reactor Dosimetry*, International Atomic Energy Agency, report IAEA-208, **Vol. 2**, 1978, pp. 265-290.

[9] J. A. Grundl, C. M. Eisenhauer, *Compendium of Benchmark Neutron Fields for Reactor Dosimetry*, National Bureau of Standards, report NBSIR 85-3151, January 1986.

[10] A. B. Pashchenko, *Reaction Cross-Sections Induced by 14.5 MeV and by Cf-252 and U-235 Fission Spectrum Neutrons: An Analytical Review*, IAEA Nuc. Data Section, rpt. INDC(CCP-323)/L, Jan. 1991.

[11] J. G. Hayes, T. B. Ryves, *Journal of Nuclear Energy*, **Vol. 8**, 1981, pp. 469-478.

[12] P. J. Griffin, J. G. Kelly, T. F. Luera, *Proceedings of the Seventh ASTM-Euratom Symposium on Reactor Dosimetry*, Kluwer Academic Publishers, 1990, pp. 669-675.

[13] *The International Reactor Dosimetry File (IRDF-90)*, assembled by N. P. Kocherov, P.K. McLaughlin, International Atomic Energy Agency, Nuclear Data Section, IAEA-NDS-141 Rev. 2, Oct. 1993.

[14] C. Y. Fu, D. M. Hetrick, *Proceedings of the Fourth ASTM-Euratom Symposium on Reactor Dosimetry: Radiation Metrology Techniques, Data Bases, and Standardization,* **Volume II**, 1982, pp. 877-887.

[15] P. J. Griffin, J. G. Kelly, T. F. Luera, *SNL RML Recommended Dosimetry Cross Section Compendium*, SAND92-0094, Sandia National Laboratories, Albuquerque, NM, 1993.

[16] P. J. Griffin, P*roceedings of the 1996 Topical Meeting Radiation Protection & Shielding: Advances and Applications in Radiation Protection and Shielding*, **Vol. 1**, April 21-25, 1996, pp. 27-35.

[17] W. Mannhart, *Handbook on Nuclear Activation Data, International Atomic Energy Agency*, Tech. Report Series #273, 1987, pp. 413-437.

[18] W. Mannhart, *Reactor Dosimetry: Methods, Applications and Standardization,* ASTM STP 1001, 1989, pp. 340-347.

[19] J. W. Boldeman, *Review of Measurements of the Prompt Neutron Spectrum From The Spontaneous Fission of Cf-252,* International Atomic Energy Agency, report IAEA-TECDOC-410.

[20] D. G. Madland, *Theory of Neutron Emission in Fission*, Los Alamos National Laboratory, Los Alamos, NM, report LA-UR-89-1747, 1989.

[21] M. Petilli, D. Gilliam, *Reactor Dosimetry*, eds. J. P. Genthon, H. Rottger, 1985, pp. 657-665.

[22] J. G. Kelly, P. J.Griffin, W. C. Fan, *IEEE Trans. on Nuclear Sci.,* **Vol. 40**, No. 6, Dec. 1993, pp. 1418.

[23] P. J. Griffin, J. G. Kelly, *IEEE Trans. on Nucl. Science,* **Vol. 42**, Dec. 1995.

[24] P. J. Griffin, J. G. Kelly, J. W. VanDenburg, *User's Manual for SNL-SAND-II Code*, SAND93-3957, Sandia National Laboratories, Albuquerque, NM, 1994.